

## RESEARCH ARTICLE

# Programmable RNA Targeting Using CasRx in Flies

Anna B. Buchman,<sup>1,†</sup> Dan J. Brogan,<sup>1,†</sup> Ruichen Sun,<sup>1,†</sup> Ting Yang,<sup>1</sup> Patrick D. Hsu,<sup>2,3</sup> and Omar S. Akbari<sup>1,4,\*†</sup>

### Abstract

CRISPR-Cas genome editing technologies have revolutionized the fields of functional genetics and genome engineering, but with the recent discovery and optimization of RNA-targeting Cas ribonucleases, we may soon see a similar revolution in the study of RNA function and transcriptome engineering. However, to date, successful proof of principle for Cas ribonuclease RNA targeting in eukaryotic systems has been limited. Only recently has successful modification of RNA expression by a Cas ribonuclease been demonstrated in animal embryos. This previous work, however, did not evaluate endogenous expression of Cas ribonucleases and only focused on function in early developmental stages. A more comprehensive evaluation of this technology is needed to assess its potential impact. Here we report on our efforts to develop a programmable platform for RNA targeting using a Cas ribonuclease, CasRx, in the model organism *Drosophila melanogaster*. By genetically encoding CasRx in flies, we demonstrate moderate transcript targeting of known phenotypic genes in addition to unexpected toxicity and lethality. We also report on the off-target effects following on-target transcript cleavage by CasRx. Taken together, our results present the current state and limitations of a genetically encoded programmable RNA-targeting Cas system in *Drosophila melanogaster*, paving the way for future optimization of the system.

### Introduction

The development of CRISPR as a programmable genome engineering tool has revolutionized the life sciences by providing transformative applications for both medicine and biotechnology.<sup>1</sup> While much of the recent focus has been on exploiting CRISPR technologies to target DNA, recent findings that certain CRISPR systems can also be programmed to target RNA have suggested new possibilities for CRISPR technologies in transcriptome engineering.<sup>2–4</sup> For example, one recent advancement was the engineering and biochemical characterization of Cas ribonuclease (CasRx) as a compact single-effector Cas enzyme that exclusively targets RNA with superior efficiency and specificity as compared to RNA interference (RNAi).<sup>4</sup> In human cells, CasRx demonstrated highly efficient on-target gene reduction with limited off-target activity, making it a potential tool for gene reduction. However, this technology has yet to be comprehensively adapted for facile use in other systems (although see<sup>5</sup>), such as *Drosophila melanogaster* (flies),

which are a common tool for exploring new biological questions and developing novel bioengineering tools *in vivo*. Non-RNAi-based techniques for reducing gene expression (without permanently altering the genome) in animals would provide for a more flexible technique to modulate gene expression in a biologically relevant way.

CasRx belongs to the Cas13 family of RNA-targeting Cas enzymes, a group of highly specific ribonucleases.<sup>4,6</sup> Though these enzymes possess promiscuous RNase activity resulting in cleavage of non-target RNA,<sup>2,4,7–9</sup> a possible drawback for applying Cas13 ribonuclease-based transcriptome engineering technologies, they may serve as a starting point for optimizing these RNA-targeting platforms for *in vivo* applications. For example, RNA-targeting CRISPR technologies could enable the development of robust gene silencing techniques in animals in which RNAi poorly functions.<sup>4,10</sup> Another potential application may involve using RNA-targeting CRISPR technologies to engineer mosquito populations resistant to infection with RNA viruses. Numerous

<sup>1</sup>Section of Cell and Developmental Biology, University of California San Diego, La Jolla, California, USA; <sup>2</sup>Laboratory of Molecular and Cell Biology, Salk Institute for Biological Studies, La Jolla, CA 92037, USA; <sup>3</sup>Helmsley Center for Genomic Medicine, Salk Institute for Biological Studies, La Jolla, California, USA; <sup>4</sup>Tata Institute for Genetics and Society, University of California, San Diego, La Jolla, California, USA.

†These authors contributed equally.

\*Address correspondence to: Omar S. Akbari, PhD, Division of Biological Sciences, Section of Cell and Developmental Biology, University of California San Diego, 9500 Gillman Drive, La Jolla, CA 92093, USA, E-mail: oakbari@ucsd.edu

This manuscript has been posted on bioRxiv (DOI: <https://doi.org/10.1101/2020.04.03.023606>).

© Anna Buchman et al. 2020; Published by Mary Ann Liebert, Inc. This Open Access article is distributed under the terms of the Creative Commons License (<http://creativecommons.org/licenses/by/4.0/>), which permits unrestricted use, distribution, and reproduction in any medium, provided the original work is properly cited.

RNA viruses of global medical importance, such as dengue, Zika, and chikungunya virus, are transmitted primarily by one species of *Aedes* mosquito. Engineering this mosquito population with virus resistance may be a tool to reduce disease transmission;<sup>11</sup> however, no current technologies have successfully targeted all of these viruses simultaneously.<sup>12–16</sup> RNA-targeting CRISPR systems may provide a platform to reduce the spread of mosquito-borne viruses by targeting viral RNA genomes in a programmable manner. Therefore, it is of high priority to further understand the utility of RNA-targeting CRISPR systems in relevant model organisms.

RNAi-based approaches are the current standard for transcriptome modification in *Drosophila*. This technology has increased our understanding of the function and regulation of many genes,<sup>10,17–20</sup> yet RNAi was reported to show occasional high false negative rates, particularly in highly expressed genes due to insufficient small RNA expression,<sup>10,17,21</sup> and at some other times high false positive rates due to positional or off-target effects.<sup>22–25</sup> Co-expression of Dicer2 can reduce false negative rates, but would in turn increase the prevalence of false positives<sup>10,17</sup> and render the entire process not as clean. Ideally, an RNA-targeting system should be easily programmable, not require expression of multiple factors, and should work in a simplified manner. CasRx, like other CRISPR systems, is easily programmable<sup>26,27</sup> and is capable of targeting nearly any coding gene, but unlike other Cas13 enzymes, it lacks a protospacer flanking sequence requirement,<sup>4</sup> making it more versatile for programmable targeting. Additionally, CasRx is a simplified RNA-targeting system as it requires no additional helper enzymes to efficiently target and degrade RNA.<sup>4</sup> For these reasons, the CasRx ribonuclease is a practical starting point for establishing a single-effector RNA-targeting platform for *in vivo* gene reduction studies. Here we report the first use of a CasRx-mediated RNA-targeting system in flies. We show that separately encoding CasRx and guide RNA arrays (gRNA<sup>array</sup>) in the genome promotes robust expression of these elements throughout development. Furthermore, we demonstrate that binary genetic crosses with ubiquitous and tissue-specific CasRx- and gRNA<sup>array</sup>-expressing fly lines can produce clear, highly penetrant phenotypes and by using RNA sequencing (RNAseq) we demonstrate that CasRx is capable of moderate targeted transcript reduction at various stages of fly development, albeit with various degrees of off-target activity. Moreover, we also found that CasRx expression and targeting was often toxic and resulted in unexpected lethality indicating further optimization will be necessary for this to be a versatile tool for *Drosophila* genetics.

## Materials and Methods

### Design and assembly of constructs

To select the CasRx target sites, target genes were analyzed to identify 30-nucleotide (nt) regions that had no poly-U stretches greater than four base pairs, had GC base content between 30% and 70%, and were not predicted to form strong RNA hairpin structures. Care was also taken to select target sites in RNA regions that were predicted to be accessible, such as regions without predicted RNA secondary or tertiary structure (Supplementary Fig. S1). All RNA folding/hairpin analysis was performed using mFold.<sup>28</sup> For transgenic gRNA arrays, four targets per gene were selected to ensure efficient targeting. We assembled four CasRx- and catalytically inactive negative control (dCasRx)-expressing constructs under the control of one of two promoters: Ubiquitin-63E (Ubiq) or the original Upstream Activation Sequence (UAS) promoter developed in Brand and Perrimon<sup>29</sup> (Ubiq-CasRx, Ubiq-dCasRx, UAS-CasRx, UAS-dCasRx) using the Gibson enzymatic assembly method.<sup>30</sup> A base vector (Addgene plasmid 112686) containing piggyBac and an attB-docking site, the Ubiq promoter fragment, SpCas9-T2A-GFP, and the Opie2-dsRed transformation marker was used as a template to build all four constructs.<sup>31</sup> To assemble constructs OA-1050E (Addgene plasmid 132416, Ubiq-CasRx), and OA-1050R (Addgene plasmid 132417, Ubiq-dCasRx), the SpCas9-T2A-GFP fragment was removed from the base vector by cutting with restriction enzymes SwaI and PacI and replaced with CasRx and dCasRx fragments amplified with primers 1050E.C3 and 1050E.C4 (Supplementary Table S1) from constructs pNLS-RfxCas13d-NLS-HA (pCasRx) and pNLS-dRfxCas13d-NLS-HA (pdCasRx),<sup>4</sup> respectively. To assemble constructs OA-1050L (Addgene plasmid 132418, UAS-CasRx) and OA-1050S (Addgene plasmid 132419, UAS-dCasRx), the base vector described above (Addgene plasmid 112686) was digested with restriction enzymes NotI and PacI to remove the Ubiq promoter and SpCas9-T2A-GFP fragments. Then the UAS promoter fragment and CasRx or dCasRx fragments were cloned in. The UAS promoter fragment was amplified from plasmid pJFRC81<sup>32</sup> using primers 1041.C9 and 1041.C11 (Supplementary Table S1). The CasRx and dCasRx fragments were amplified with primers 1050L.C1 and 1050E.C4 (Supplementary Table S1) from constructs pCasRx and pdCasRx, respectively.

We designed four constructs, each carrying a four-gRNA array: OA-1050G (Addgene plasmid 132420), OA-1050I (Addgene plasmid 132421), OA-1050J (Addgene plasmid 133304), and OA-1050Z4 (Addgene plasmid 132425), targeting transcripts of *white*, *Notch*, *GFP*, and

*yellow*, respectively. To generate a base plasmid, OA-1043, which was used to build all constructs carrying the four-gRNA array, Addgene plasmid 112688 containing the *miniwhite* gene as a marker, an attB-docking site, a *D. melanogaster* polymerase-3 U6 (U6:3) promoter fragment, and a gRNA fragment with a target, scaffold, and terminator sequence was digested with restriction enzymes AscI and XbaI to remove the U6:3 promoter and gRNA fragments. Then, the U6:3 promoter fragment was amplified from the same Addgene plasmid 112688 with primers 1043.C1 and 1043.C23 (Supplementary Table S1) and was cloned back using Gibson enzymatic assembly. To generate constructs OA-1050G, OA-1050I, and OA-1050Z4, plasmid OA-1043 was digested with restriction enzymes PstI and NotI. Then, a fragment that contained arrays of four tandem variable gRNAs (comprised of a 36-nt direct repeat [DR] and a 30-nt spacer) corresponding to different target genes followed by an extra DR and a seven-thymine terminator was synthesized and subcloned into the digested backbone using Gene Synthesis (GenScript USA, Inc.). To generate construct OA-1050J, a fragment containing arrays of four tandem variable gRNAs targeting *GFP* with an extra DR and a seven-thymine terminator followed by the OpIE2-GFP marker was synthesized and subcloned into the above digested OA-1043 backbone using Gene Synthesis (GenScript USA, Inc.). We have also made all plasmids and sequence maps available for download and/or order from Addgene using the identification numbers listed in Supplementary Fig. S2 and Supplementary Table S2.

### Fly genetics and imaging

Flies were maintained under standard conditions at 26°C. Embryo injections were performed at Rainbow Transgenic Flies, Inc.. All CasRx and dCasRx-expressing lines were generated by site-specifically integrating our constructs at available  $\phi$ C31 integration sites on the 2nd chromosome (sites 8621 [UAS/-(d)CasRx] and attp40w [Ubiq-(d)CasRx]). Homozygous lines were established for UAS-CasRx and UAS-dCasRx, and heterozygous balanced lines were established for Ubiq-CasRx and Ubiq-dCasRx (over Curly of Oster: CyO). All gRNA<sup>array</sup>-expressing lines were generated by site-specific integrating constructs at an available  $\phi$ C31 integration site on the third chromosome (site 8622). Homozygous lines were established for all gRNA<sup>array</sup>-expressing flies.

To genetically assess the efficiency of CasRx ribonuclease activity, we bidirectionally crossed Ubiq-CasRx- and Ubiq-dCasRx-expressing lines to gRNA<sup>array</sup>-expressing lines at 26°C. F<sub>1</sub> transheterozygotes were scored for the inheritance and penetrance of observable phenotypes.

Embryo, larvae, and pupae counts were preceded by crossing male Ubiq-CasRx- or Ubiq-dCasRx-expressing flies to female gRNA<sup>array</sup>-expressing flies. Flies were incubated at 26°C for 48 h with yeast to induce embryo laying. Flies were then transferred to embryo collection chambers containing yeast-smear grape-juice plates and were incubated at 26°C overnight (16 h). The grape-juice plates were then removed, the embryos were counted, and the grape-juice plates were incubated for 24 h at 26°C. Total larvae and transheterozygote larvae were then counted, and the grape-juice plates were transferred to jars and incubated at 26°C. Once all larvae reached the pupal stage, total, and transhet pupae were counted. Finally, total adult flies and total adult transheterozygotes were counted 20 days post initial lay. Each genetic cross was set using 5 male and 10 female (paternal CasRx) or 4 male and 8 female (maternal CasRx) flies in triplicate.

To investigate the tissue-specific activity of CasRx, we designed a two-step crossing scheme to generate F<sub>2</sub> triple transheterozygotes (Fig. 1A). First, we crossed double-balanced UAS-CasRx- or UAS-dCasRx-expressing flies (male) to homozygous gRNA<sup>array</sup>-expressing flies (female) to generate F<sub>1</sub> transheterozygote males carrying the TM6-balancer chromosome. The F<sub>1</sub> transheterozygote males carrying TM6 were then crossed with a Gal4-driver-expressing line. F<sub>2</sub> triple transheterozygous inheritance and phenotype penetrance was scored based on visible phenotypes manifesting in flies F<sub>2</sub> flies with red eyes, a lack of the TM6 balancer chromosome, and red fluorescent protein (dsRed) expression. Marked by the presence of dsRed (for UAS-CasRx or UAS-dCasRx), red eyes (to mark the gRNA), and the lack of TM6, F<sub>2</sub> triple transheterozygotes' inheritance and phenotype penetrance was scored. Each cross was set using 1 female and 10 male flies in triplicate. The flies were imaged on the Leica M165FC fluorescent stereomicroscope equipped with a Leica DMC4500 color camera. Image stacks of adult flies were taken in Leica Application Suite X (LAS X) and compiled in Helicon Focus 7. Stacked images were then cropped and edited in Adobe Photoshop CC 2018.

### Illumina RNA sequencing

The total RNA was extracted from F<sub>1</sub> transheterozygous flies at different developmental stages based on the expression data available through modENCODE analysis (Supplementary Fig. S3). For guide RNA targeting the *white* gene (gRNA<sup>w</sup>) flies, transheterozygous adult heads were removed one day after emerging and were frozen at -80°C. For guide RNA targeting the *yellow* gene (gRNA<sup>y</sup>) flies, the flies were incubated in vials for 48 h with yeast to induce embryo laying. The flies were then

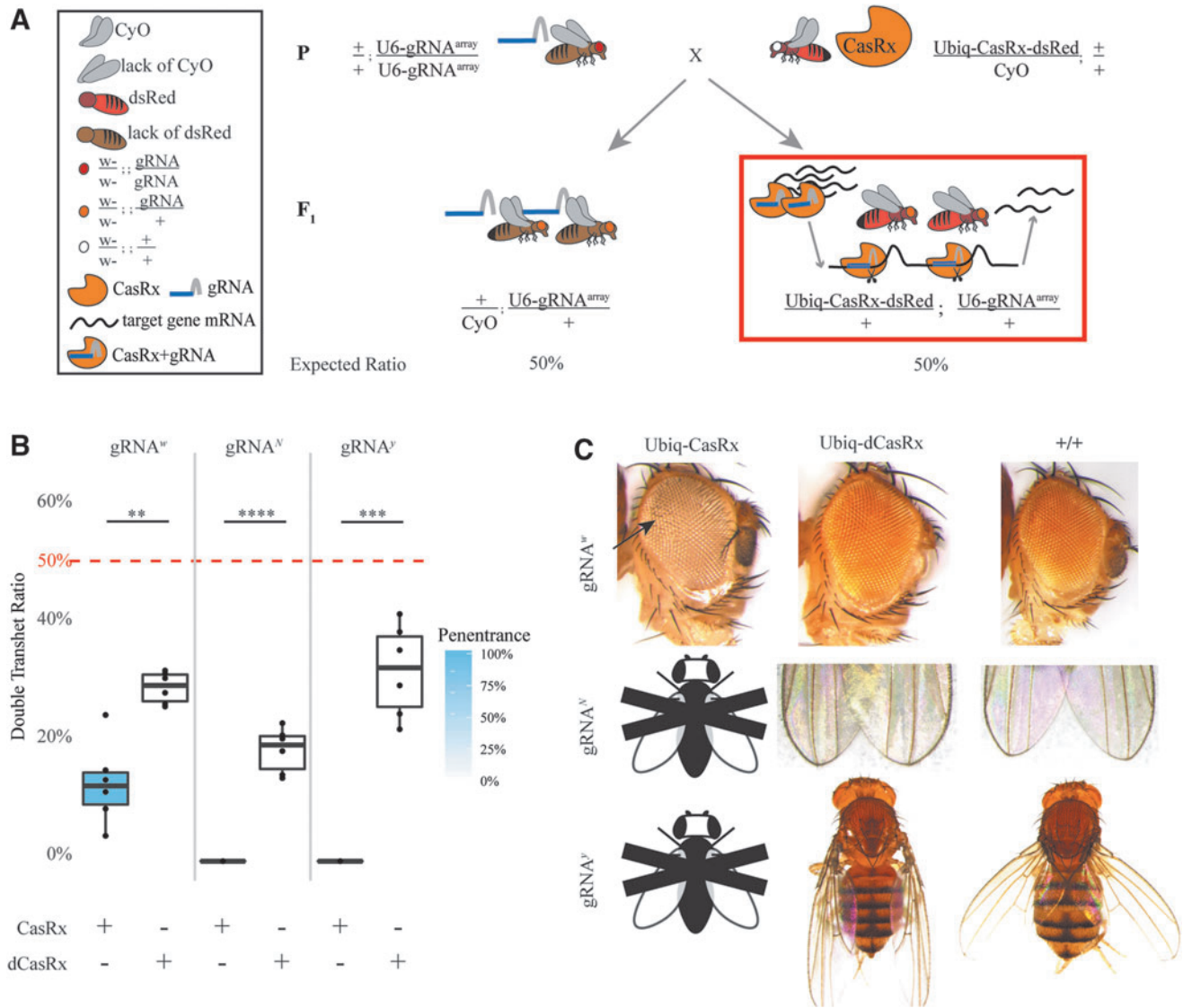


**Fig. 1.** CasRx-mediated target transcript reduction in restricted tissue types using the binary Gal4/UAS system. **(A)** Representative genetic crossing schematic. **(B)** Inheritance rates of triple transheterozygous flies inheriting three transgenes (UAS-CasRx or UAS-dCasRx, gRNA<sup>array</sup>, and Gal4-driver), corresponding to flies highlighted in the red box in panel A. Significant differences in inheritance between CasRx and dCasRx groups were observed in all three gene targets (gRNA<sup>w</sup>,  $P=0.00595$ ; gRNA<sup>N</sup>,  $P=0.00402$ ; gRNA<sup>y</sup>,  $P=0.02205$ ). **(C)** Phenotypes of the triple transheterozygous flies. The white arrow identifies chitin pigment reduction in the thorax resulting from *y* targeting. Black and white fly with “X” represents a lethal phenotype with no live adults able to be scored or imaged. CasRx, Cas ribonuclease; gRNA<sup>array</sup>, guide RNA array; gRNA<sup>N</sup>, guide RNA targeting the *Notch* gene; gRNA<sup>w</sup>, guide RNA targeting the *white* gene; gRNA<sup>y</sup>, guide RNA targeting the *yellow* gene.

transferred to embryo collection chambers containing yeast-smear grape-juice plates and incubated at 26°C for 3 h. The flies were then removed, and the embryos were aged on the grape-juice plates (gRNA<sup>y</sup> = 17 h; 17–20 h total). The embryos were removed from the grape-juice plates, washed with deionized H<sub>2</sub>O, and frozen at –80°C. The guide RNA targeting the *Notch* gene

(gRNA<sup>N</sup>) and guide RNA targeting the *Green Fluorescent Protein* gene (gRNA<sup>GFP</sup>) flies were incubated in vials with yeast for 48 h to induce embryo laying. The flies were then transferred to a new vial and allowed to lay overnight (16 h). The adults were removed, and the vials were incubated at 26°C for 24 h. Transheterozygote first instar larvae were then picked (based on dsRed expression) and

frozen at  $-80^{\circ}\text{C}$ . For all samples, the total RNA was extracted using Qiagen RNeasy Mini Kit (Qiagen 74104). Following extraction, the total RNA was treated with Invitrogen Turbo<sup>TM</sup> DNase (Invitrogen AM2238). The RNA concentration was analyzed using a Nanodrop One<sup>C</sup> UV-vis spectrophotometer (ThermoFisher ND-ONEC-W). The RNA integrity was assessed using an RNA 6000 Pico Kit for Bioanalyzer (Agilent Technologies 5067-1513). The RNA-seq libraries were constructed using NEBNext Ultra II RNA Library Prep Kit for Illumina (NEB E7770) following the manufacturer's instructions.<sup>33</sup> The libraries were sequenced on an Illumina HiSeq2500 in single read mode with a read length of 50 nt and a sequencing depth of 20 million reads per library following the manufacturer's instructions. Base calls were performed with RTA 1.18.64 followed by conversion to FASTQ with bcl2fastq 1.8.4. We sequenced and analyzed three replicates for all CasRx and dCasRx samples. In total, we sequenced and analyzed 24 samples: 12 CasRx experimental samples and 12 dCasRx control samples. All raw sequencing data can be accessed at the National Center for Biotechnology Information Sequence Read Archive (NCBI SRA; submission ID SUB6818910 [BioProject PRJNA600654]).

#### Bioinformatics: Quantification and differential expression analysis

Reads were mapped to the *D. melanogaster* genome (BDGP release 6; GenBank accession GCA\_000001215.4) supplemented with cDNA sequences of CasRx and GFP using the default parameters of STAR aligner<sup>34</sup> with the addition of the “-outFilterType BySJout” filtering option and “-sjdbGTFfile *Drosophila\_melanogaster*.BDGP6.22.97.gtf” gene transfer format (GTF) file downloaded from ENSEMBL. The expression levels were determined with featureCounts<sup>35</sup> using “-t exon -g gene\_id -M -O -fraction” options. The raw transcript counts were normalized to transcripts per million (TPM), which were calculated from count data using the “addTpmFpkmToFeatureCounts.pl” Perl script (see Supplementary Material, Supplementary File S1). The raw count and TPM data are available in Supplementary Tables S3 and S4. To further explore CasRx-induced differential gene expression profiles, we used the maximum *a posteriori* method with the original shrinkage estimator in the DESeq2 pipeline to estimate the transcript logarithmic fold change.<sup>36</sup> The Wald test with the Benjamini-Hochberg correction was used for statistical inference. The analysis script can be found in the Supplementary Material (Supplementary File S2), and the analyzed results are in Supplementary Tables S5–S9. Per the DESeq2 analysis requirements,

some values are shown as NA (not applicable) for the following reasons: (1) if all samples for a given transcripts have 0 transcript counts, this transcript's baseMean will be 0 and its logarithmic fold change, *P* value, and padj will be set to NA; (2) if one replicate of a transcript is an outlier with an extreme count (detected by Cook's distance), this transcript's *P* value and padj will be set to NA; or (3) if a transcript is found to have a low mean normalized count after automatic independent filtering, this transcript's padj will be set to NA.

## Results

### Genetically encoding CasRx in flies

To genetically determine the RNA-targeting capabilities of CasRx, *in vivo*, we engineered flies encoding two versions of the CasRx ribonuclease: the active enzyme and a catalytically inactive negative control (dCasRx). We did this by generating transgenes that use a broadly expressing ubiquitin (Ubiq) promoter<sup>37</sup> to drive expression of either CasRx (Ubiq-CasRx) or dCasRx (Ubiq-dCasRx) (Supplementary Fig. S2). CasRx exhibits two distinct RNase activities for processing its cognate gRNA<sup>array</sup> and cleaving target RNA. Because we wanted our negative control to still bind target RNA and efficiently process the gRNA<sup>array</sup>, we eliminated programmable RNA cleavage in dCasRx by inactivating the positively charged catalytic residues of the HEPN motifs.<sup>4</sup> We established these transgenic lines by integrating each transgene site-specifically using an available  $\phi\text{C31}$  docking site located on the second chromosome (atp40w) (Supplementary Fig. S2; Supplementary Table S2). These flies were viable, though we were unable to generate homozygotes for either CasRx or dCasRx, presumably due to high levels of ubiquitously ribonuclease expression. While homozygotes are desirable because, when outcrossed, all progeny would receive a copy of the transgene, we were still able to assess CasRx activity by maintaining these stocks as heterozygotes balanced over the chromosome Curly-of-Oster (CyO), which ensures a non-lethal expression level of CasRx while retaining the transgene (Supplementary Table S2). To genetically measure the efficacy of programmable RNA targeting, we targeted three genes known to produce visible phenotypes when expression is disrupted, including: *white* (*w*), *Notch* (*N*), and *yellow* (*y*).<sup>38–41</sup> To target these genes with CasRx, we designed a gRNA<sup>array</sup> for each gene driven by a ubiquitously expressed polymerase-3 U6 (U6:3) promoter<sup>31,42</sup> (Supplementary Fig. S2; Supplementary Table S2). Each array consisted of four transcript-targeting spacers (30 nt in length) each positioned between CasRx-specific direct repeats (36 nt in length) with a conserved 5'-AAAAC motif designed to be processed by either CasRx or dCasRx<sup>4</sup> (Supplementary

Fig. S2). For each gRNA<sup>array</sup>, we site-specifically integrated the transgene at an available  $\phi$ C31 docking site located on the third chromosome (site 8622) and established a homozygous transgenic line (Supplementary Fig. S2; Supplementary Table S2).

### Programmable RNA targeting of endogenous target genes

To assess the efficacy of programmable RNA targeting by CasRx, we conducted bidirectional genetic crosses between homozygous gRNA<sup>array</sup> (+/+; gRNA<sup>array</sup>/gRNA<sup>array</sup>) expressing flies crossed to either Ubiq-CasRx (Ubiq-CasRx/CyO; +/+) or Ubiq-dCasRx (Ubiq-dCasRx/CyO; +/+) expressing flies (Fig. 2A). When crossed to Ubiq-CasRx, we were able to obtain highly penetrant (100%) expected visible eye pigmentation disruption phenotypes exclusively in transheterozygotes (Ubiq-CasRx/+; gRNA<sup>array</sup> /+) for *w* suggesting that CasRx exhibits programmable on-target RNA cleavage capabilities (Fig. 2B and C; Supplementary Table S10). However, while we expected Mendelian transheterozygote inheritance rates to be 50%, the recorded inheritance rates were significantly lower than expected (12.9%), suggesting some degree of unexpected toxicity leading to lethality (Fig. 2B; Supplementary Fig. S4; Supplementary Table S10). Moreover, when targeting *y* or *N*, Ubiq-CasRx transheterozygotes (Ubiq-CasRx/+; gRNA<sup>array</sup> /+) were 100% lethal and did not develop beyond the second instar larval stage (Supplementary Fig. S5A and C). This was expected for *N* as there are many examples of lethal alleles for this gene;<sup>43–45</sup> however, mutations in *y* should be recessive viable with defective chitin pigmentation producing yellow cuticle phenotypes.<sup>36</sup> It is worth noting that the corresponding Ubiq-dCasRx transheterozygote controls also showed less than 50% inheritance rates, though less severe than the Ubiq-CasRx transheterozygote experimental group. This indicates that the CasRx system may introduce toxicity when expressed at the organismal level. Furthermore, we were unable to obtain visual phenotypes in transheterozygotes (Ubiq-dCasRx/+; gRNA<sup>array</sup> /+) from our negative control crosses using all arrays tested, indicating that a catalytically active form of the ribonuclease is necessary for visual phenotypes to be observed (Fig. 2C). Taken together, these results indicate that the catalytically active form of the CasRx ribonuclease can generate phenotypes, although unexpected toxicity which resulted in lethality (only in the presence of the CasRx and the array) were also observed.

### Tissue-Specific RNA Targeting by CasRx

Given the above toxicity when ubiquitously expressed, we next explored the efficiency of CasRx when expres-

sion was restricted to specific cell types and tissues. We leveraged the classical binary Gal4/UAS system which enables targeted gene expression.<sup>29</sup> To develop this system, we generated two transgenes using the UAS promoter<sup>29</sup> to drive expression of either CasRx (UAS-CasRx) or dCasRx (UAS-dCasRx) as a negative control (Supplementary Fig. S2). These transgenes were integrated site-specifically using a  $\phi$ C31 docking site located on the second chromosome (site 8621), and these stocks were homozygous viable (Supplementary Fig. S2; Supplementary Table S2). To activate CasRx expression in specific tissues, we used available Gal4 driver lines that restricted expression to either the eye (GMR-Gal4)<sup>46</sup> or the wing and body (yellow-Gal4);<sup>47</sup> (Supplementary Table S2). These lines were crossed to the same homozygous gRNA<sup>array</sup> lines described above targeting *w*, *y*, or *N* (Supplementary Fig. S2; Supplementary Table S2). To test this system, we performed a two-step genetic crossing scheme to generate F<sub>2</sub> triple transheterozygotes (either UAS-CasRx/+; gRNA<sup>array</sup>/Gal4 or UAS-dCasRx/+; gRNA<sup>array</sup>/Gal4) (Fig. 1A). This consisted of initially crossing homozygous gRNA<sup>array</sup> (gRNA<sup>array</sup>/gRNA<sup>array</sup>) expressing flies to heterozygous, double-balanced UAS-CasRx (UAS-CasRx/CyO; TM6/+) flies, or for the negative control, heterozygous, double-balanced UAS-dCasRx (UAS-dCasRx/CyO; TM6/+) flies. The second step was to cross the F<sub>1</sub> transheterozygote males expressing both a CasRx ribonuclease and the gRNA<sup>array</sup> (UAS-CasRx/+; gRNA<sup>array</sup>/TM6 or UAS-dCasRx/+; gRNA<sup>array</sup>/TM6) to respective homozygous Gal4 driver lines to generate F<sub>2</sub> triple transheterozygotes (UAS-CasRx/+; gRNA<sup>array</sup>/Gal4 or UAS-dCasRx/+; gRNA<sup>array</sup>/Gal4) to be scored for phenotypes (Fig. 1A).

From these crosses, our results indicated that tissue-specific expression of CasRx can indeed result in phenotypes, though this was also accompanied by tissue-specific cell death or organismal lethality, similar to previous observations of ubiquitous CasRx expression described above. For example, of the expected 25% Mendelian inheritance rates from the F<sub>1</sub> cross between gRNA<sup>w</sup> (UAS-CasRx/+; gRNA<sup>w</sup>/TM6) and GMR-Gal4 (+/+; GMR-Gal4/GMR-Gal4), we observed survival of only 0.57% viable F<sub>2</sub> triple transheterozygotes (UAS-CasRx/+; gRNA<sup>w</sup>/GMR-Gal4), all of which displayed severe eye specific pigmentation and morphology phenotypes (Fig. 1B and C; Supplementary Fig. S6; Supplementary Table S11). This gRNA<sup>w</sup> F<sub>2</sub> triple transheterozygote inheritance rate was significantly lower than the corresponding negative control F<sub>2</sub> triple transheterozygote (UAS-dCasRx/+; gRNA<sup>w</sup>/GMR-Gal4) inheritance rate, which was closer to the expected 25% Mendelian inheritance (27.6%) (Supplementary Fig. S6; Supplementary Table S11). Moreover, using the same

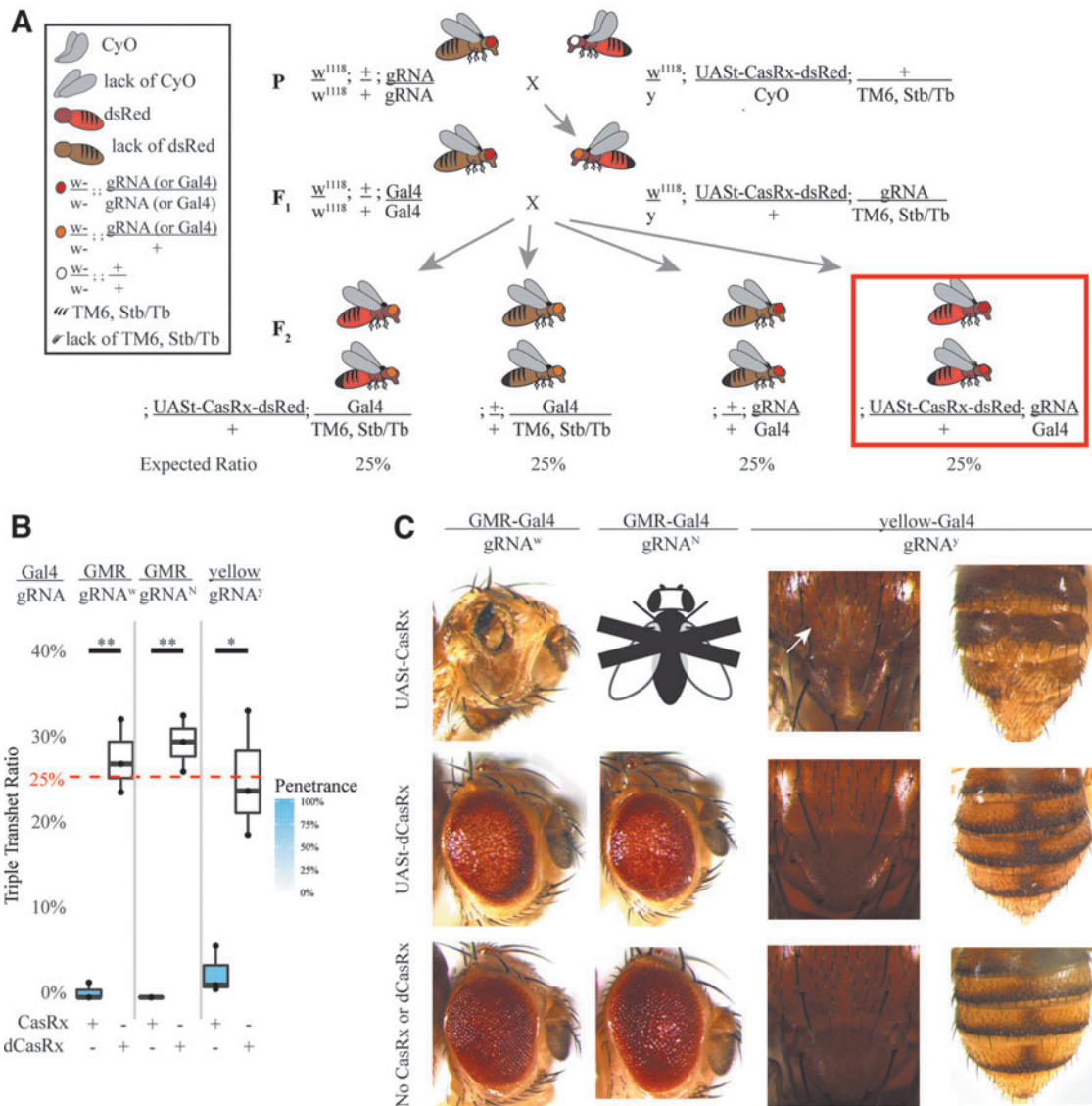


**Fig. 2.** Genetic assessment of programmable CasRx-mediated transcript reduction in flies. **(A)** Representative genetic crossing schematic to generate transheterozygotes. **(B)** Inheritance and penetrance rates of transheterozygous flies inheriting both Ubiq-CasRx (or Ubiq-dCasRx) and  $gRNA^{array}$  corresponding to the red box in panel A. Phenotype penetrance rate is depicted by blue shading in the box plot. Significant differences in inheritance between CasRx and dCasRx groups were observed in all three groups ( $P$  values:  $gRNA^w = 0.00135$ ;  $gRNA^N = 0.00006$ ;  $gRNA^Y = 0.00016$ ). **(C)** Brightfield images of transheterozygous flies with representative phenotypes for each cross. Corresponding genotype for each image is dictated by the combination of constructs on top of the columns and the side of the rows. Arrows point to tissue necrosis in the eye. Black and white fly with "X" represents lethality phenotype where no transheterozygote adults emerged. dCasRx, catalytically inactive negative control CasRx.

Gal4 driver (GMR-Gal4), a significant difference in inheritance was also observed for  $N$  targeting, which resulted in 100% lethality in  $F_2$  triple transheterozygotes (UAS-CasRx/+;  $gRNA^N$ /GMR-Gal4) compared to the 29.3% inheritance rate for the negative control  $F_2$  triple transheterozygotes (UAS-dCasRx/+;  $gRNA^N$ /GMR-

Gal4) (Fig. 1B and C; Supplementary Fig. S6; Supplementary Table S11). Finally, when targeting  $y$  using the yellow-Gal4 driver (+/+;  $y$ -Gal4/ $y$ -Gal4), we observed marginal chitin pigment reduction as small patches of yellow cuticle on the thorax and abdomen in  $F_2$  triple transheterozygotes (UAS-CasRx/+;  $gRNA^Y$ / $y$ -Gal4)

(Fig. 1C, arrows) which is a phenotype that would be expected when *y* is disrupted. Similar to crosses described above, the F<sub>2</sub> triple transheterozygote (UAS-CasRx/+; gRNA<sup>y</sup>/y-Gal4) inheritance was significantly lower (2.67%) when compared to the control F<sub>2</sub> triple transheterozygote (UAS-dCasRx/+; gRNA<sup>y</sup>/y-Gal4) inheritance (25.2%), indicating a substantial degree of lethality (Fig. 1B and C; Supplementary Fig. S6; Supplementary Table S11). In all negative control crosses, phenotypes were not observed in F<sub>2</sub> triple transheterozygotes (UAS-dCasRx/+; gRNA<sup>array</sup>/Gal4) again indicating that functional catalytic residues of the HEPN motifs are necessary for generating phenotypes observed (Fig. 2B and C; Supplementary Table S11). Taken together, these results demonstrate that tissue-specific expression of CasRx using the classical Gal4/UAS approach can result in phenotypes. However, as seen in the ubiquitous binary approach above, toxicity and lethality phenotypes were also observed again limiting the utility of the system.

#### Criteria for CasRx-mediated phenotypes

Because CasRx on-target cleavage resulted in unexpected lethality we set out to determine the importance of target sequence availability to CasRx-mediated lethality. To do so, we opted to target a gene that is not natively expressed in flies. Therefore, we generated a green fluorescent protein (GFP) reporter assay to assess the necessity of a target sequence in CasRx-mediated lethality while simultaneously visualizing on-target transcript reduction. We designed a binary GFP reporter construct consisting of both a CasRx gRNA<sup>array</sup> targeting GFP along with GFP expression driven by the broadly expressing OpIE2 promoter (gRNA<sup>GFP</sup>) (Fig. 3; Supplementary Fig. S2; Supplementary Table S2).<sup>48</sup> We established a homozygous transgenic line (+/+; gRNA<sup>GFP</sup>-OpIE2-GFP/gRNA<sup>GFP</sup>-OpIE2-GFP) by site-specifically integrating the construct at an available  $\phi$ C31 docking site located on the 3rd chromosome (site 8622) (Supplementary Fig. S2; Supplementary Table S2). To test for GFP transcript targeting, we performed bidirectional crosses between homozygous flies expressing gRNA<sup>GFP</sup> (+/+; gRNA<sup>GFP</sup>-OpIE2-GFP/gRNA<sup>GFP</sup>-OpIE2-GFP) to heterozygous Ubiqu-CasRx-expressing flies (Ubiqu-CasRx/CyO; +/+) or heterozygous Ubiqu-dCasRx-expressing flies (Ubiqu-dCasRx/CyO; +/+) as a negative control (Fig. 3A). With this assay, we observed 100% larval lethality for F<sub>1</sub> transheterozygotes (Ubiqu-CasRx/+; gRNA<sup>GFP</sup>-OpIE2-GFP/+), while larval lethality was eliminated in F<sub>1</sub> progeny that did not inherit Ubiqu-CasRx (CyO/+; gRNA<sup>GFP</sup>-OpIE2-GFP/+ in addition to the transheterozygote controls (Ubiqu-dCasRx/+; gRNA<sup>GFP</sup>-OpIE2-GFP/+). Lethality was also observed regardless of the maternal or paternal depo-

sition of CasRx (Fig. 3B; Supplementary Table S10). Given that GFP expression was also visible in larvae, we monitored the development of the F<sub>1</sub> progeny and observed that Ubiqu-CasRx transheterozygotes survived only to the first instar developmental stage, but not beyond (Supplementary Fig. S5). Given this survival, we imaged first instar transheterozygote (Ubiqu-CasRx/+; gRNA<sup>GFP</sup>-OpIE2-GFP/+ larvae and observed near-complete reduction in GFP expression for Ubiqu-CasRx transheterozygote larvae as compared to Ubiqu-dCasRx transheterozygote (Ubiqu-dCasRx/+; gRNA<sup>GFP</sup>-OpIE2-GFP/+) control larvae indicating robust CasRx mediated target transcript (GFP) reduction (Fig. 3C). Taken together, these results suggest that CasRx possesses programmable RNA-targeting activity, and the lethality is dependent upon the availability of a guide RNA and a target sequence as well as enzymatic RNA cleavage mediated by the positively charged residues of CasRx HEPN domains.

#### Quantification of CasRx-mediated on/off-target activity

We next aimed to quantify both the on- and potential off-target transcript reduction rates. To do this, we analyzed all gRNA<sup>array</sup> target genes from our binary crosses producing either highly penetrant, visible phenotypes (*w*) or lethal phenotypes (*N*, *y*, and *GFP*) (Supplementary Table S12). To do so, we implemented whole-transcriptome RNAseq analysis comparing F<sub>1</sub> Ubiqu-CasRx transheterozygotes (Ubiqu-CasRx/+; gRNA<sup>array</sup> /+) to control F<sub>1</sub> Ubiqu-dCasRx transheterozygotes (Ubiqu-dCasRx/+; gRNA<sup>array</sup> /+) (Fig. 2A, red box; Fig. 3A, red box; Supplementary Table S12). Using the available transcriptome data of *D. melanogaster* (modENCODE),<sup>49</sup> we extracted total RNA stages of development when high transcript expression levels were expected for each target gene with the exception of *GFP*, where we sequenced first instar larvae (Supplementary Fig. S3; Supplementary Table S12). In total, we analyzed 24 samples (Supplementary Table S12). From our bioinformatic analysis, we found reduced target transcript expression (Fig. 4A and B). For example, of the four target genes, CasRx was able to target and significantly reduce (1.5%–2.9%; Supplementary Table S13) the target transcript expression of three genes compared with dCasRx controls *N*, *y*, and *GFP* (Fig. 4B; Supplementary Tables S3–S9). Although we did not observe significant transcript reduction targeting *w* we did consistently observe relative expression reduction by comparing Ubiqu-CasRx samples to Ubiqu-dCasRx controls, indicating some degree of on-target reduction which likely contributes to the phenotypes observed (Fig. 4B; Supplementary Tables S3–S9). We also quantified the number of genes with significantly misexpressed transcripts by



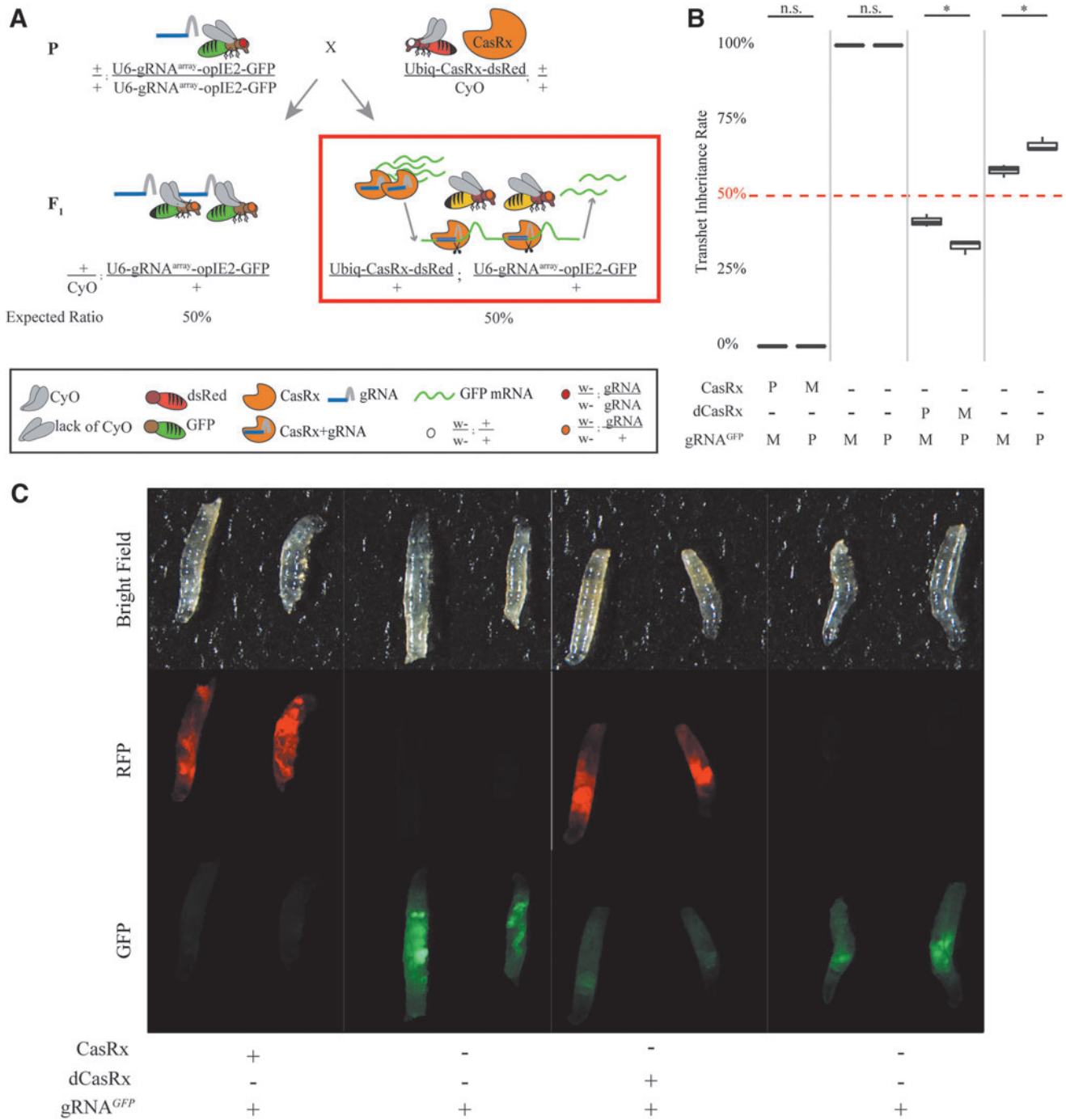


**Fig. 3.** Robust CasRx-mediated reduction of GFP. **(A)** Representative bidirectional genetic crossing schematic. **(B)** Box plot of transheterozygote inheritance rates resulting from bidirectional crosses between Ubiq-CasRx (or Ubiq-dCasRx) and gRNA<sup>GFP</sup>-OpIE2-GFP flies. **(C)** Images of F<sub>1</sub> larvae from paternal crosses demonstrating significant reduction in GFP expression for transheterozygous larvae expressing both Ubiq-CasRx and gRNA<sup>GFP</sup>-OpIE2-GFP compared to control transheterozygotes expressing Ubiq-dCasRx and gRNA<sup>GFP</sup>-OpIE2-GFP or without expressing a CasRx protein. (Left-right) Ubiq-CasRx/gRNA<sup>GFP</sup> transheterozygous larvae, heterozygous gRNA<sup>GFP</sup> larvae from Ubiq-CasRx cross, Ubiq-dCasRx/gRNA<sup>GFP</sup> transheterozygous larvae, heterozygous gRNA<sup>GFP</sup> larvae from Ubiq-dCasRx cross. CyO, ; dsRed, red fluorescent protein; GFP, green fluorescent protein; M, maternal inheritance of CasRx; P, paternal inheritance of CasRx; RFP, red fluorescent protein.

comparing Ubiq-CasRx to Ubiq-dCasRx using DESeq2<sup>50</sup> (Fig. 4A, red dots; Supplementary Tables S5–S9).

Across all gene targets, we observed some evidence of potential off-target activity, which we define as significantly misexpressed genes between CasRx and dCasRx samples. The observed potential off-target activity was demonstrated by significant changes in the gene-expression levels of numerous non-target transcripts. The number of significantly differentially expressed non-target transcripts in each group are: 253 (*w*), 300 (*N*), 41 (*y*), and 5,880 (*GFP*), representing 1.4% (*w*), 1.7% (*N*), 0.23% (*y*), and 33% (*GFP*) of the total transcripts (Fig. 4A and C; Supplementary Tables S5–S9). Taking a closer look at the gene-expression profiles of the four gene targets, we found that a total of 6,082 transcripts (out of 17,779) displayed significant expression level changes in at least one of the six CasRx-expressing groups compared to their corresponding dCasRx-expressing control group (Supplementary Tables S5–S9). Among the 6,082 misexpressed transcripts, 5,722 transcripts are affected by only one of the four genes targeted when CasRx is present, 334 transcripts are affected by two gene targets, 20 transcripts are affected by three gene targets, and 6 transcripts are affected by four gene targets simultaneously (Supplementary Tables S5–S9). As targeting exogenously introduced GFP induces 33% of the endogenous transcripts to be misexpressed, suggesting that at the organismal level CasRx system has the risk of resulting in high off-target activity and collateral tissue damages resulting in observed lethality. This quantitative analysis of CasRx-mediated transcript reduction provides evidence of CasRx ribonuclease capabilities in flies, while also identifying potential off-target effects resulting in significantly misexpressed non-target genes. That said, it should be emphasized that these off-target results should be taken with a grain of salt as we are unable to tease apart pleiotropic effects that could also contribute to misexpression of non-target transcripts and therefore a more comprehensive characterization of CasRx mediated off-targets should be conducted in the future.

## Discussion

Our results demonstrate that CasRx has some potential for programmable RNA targeting in flies, as we did observe some expected phenotypes for each target transcript, including *GFP* (lethality; reduction in *GFP* expression), *N* (lethality), *y* (lethality; yellow patches on cuticle and thorax) and *w* (white eyes and necrosis in eyes for Gal4). Specifically, RNA targeting was demonstrated with ubiquitous, inducible, and tissue-specific CasRx expression systems against native and synthetic RNA targets, which are prerequisites for enabling com-

prehensive studies of gene function. However, we did also consistently observe both cellular toxicity from the ubiquitous expression of CasRx and dCasRx as we could not generate homozygous strains for either, and unexpected lethality and tissue necrosis, presumably due collateral off target effects which have been a feature previously observed for many CRISPR ribonucleases including CasRx.<sup>2,4,7–9,51</sup> Nevertheless, in both bidirectional and Gal4/UAS crosses, we were able to obtain visible phenotypes as well as quantitative evidence (e.g., RNAseq data demonstrating a reduction in target gene expression) indicating that the CasRx is capable of targeting and degrading target RNA in flies. It is interesting to note that for one of the targeted genes (*w*), while the observed phenotype indicated consistent on-target transcript reduction, DESeq2 analysis did not reveal significant on-target reduction, which may be due to the timing of sample collection for RNAseq since expression levels of these genes vary over development.

Notwithstanding, we were able to obtain expected visual phenotypes in addition to significant on-target CasRx mediated transcript reduction for three of the targeted genes: *y*, *N*, and *GFP*. Interestingly, transheterozygotes (Ubiq-CasRx/+; gRNA<sup>array</sup> /+) for *y*, *N*, and *GFP* also had many other misexpressed non-target genes, possibly indicating that target cleavage results in increased collateral off-target activity that is detrimental to development as these individuals were adult lethal. For example, targeting *GFP*, a nonessential gene, produced the largest number of misexpressed genes as well as the most significant fold change in expression compared to all other gene targets analyzed. Additionally, because *Gadd45*, a gene involved in cellular arrest and apoptosis in *D. melanogaster*,<sup>52</sup> was also significantly misexpressed in four samples (*w*, *N*, *y*, and *GFP*) (Supplementary Tables S5–S9), it is possible that CasRx cleavage may result in an increased level of misexpressed genes leading to lethality or cellular apoptosis. Moreover, for the off target analysis for most of the target genes less than 300 (1.7%) other genes were misexpressed, however for GFP we found 5880 (33%) of genes misexpressed and it remains unclear whether this is a result of guide specific off-target, pleiotropic effects, or simply bystander cleavage (i.e. collateral off targeting).

Through this study, we identified two main factors contributing to CasRx-mediated lethality: (i) the catalytic activity of the CasRx HEPN domains, as lethality and tissue necrosis phenotypes were eliminated in dCasRx compared to CasRx crosses, and (ii) the presence of the guide RNA and target transcript resulting in on-target cleavage, as lethality was only observed when crossing Ubiq-CasRx-expressing flies to gRNA<sup>GFP</sup>-expressing flies.

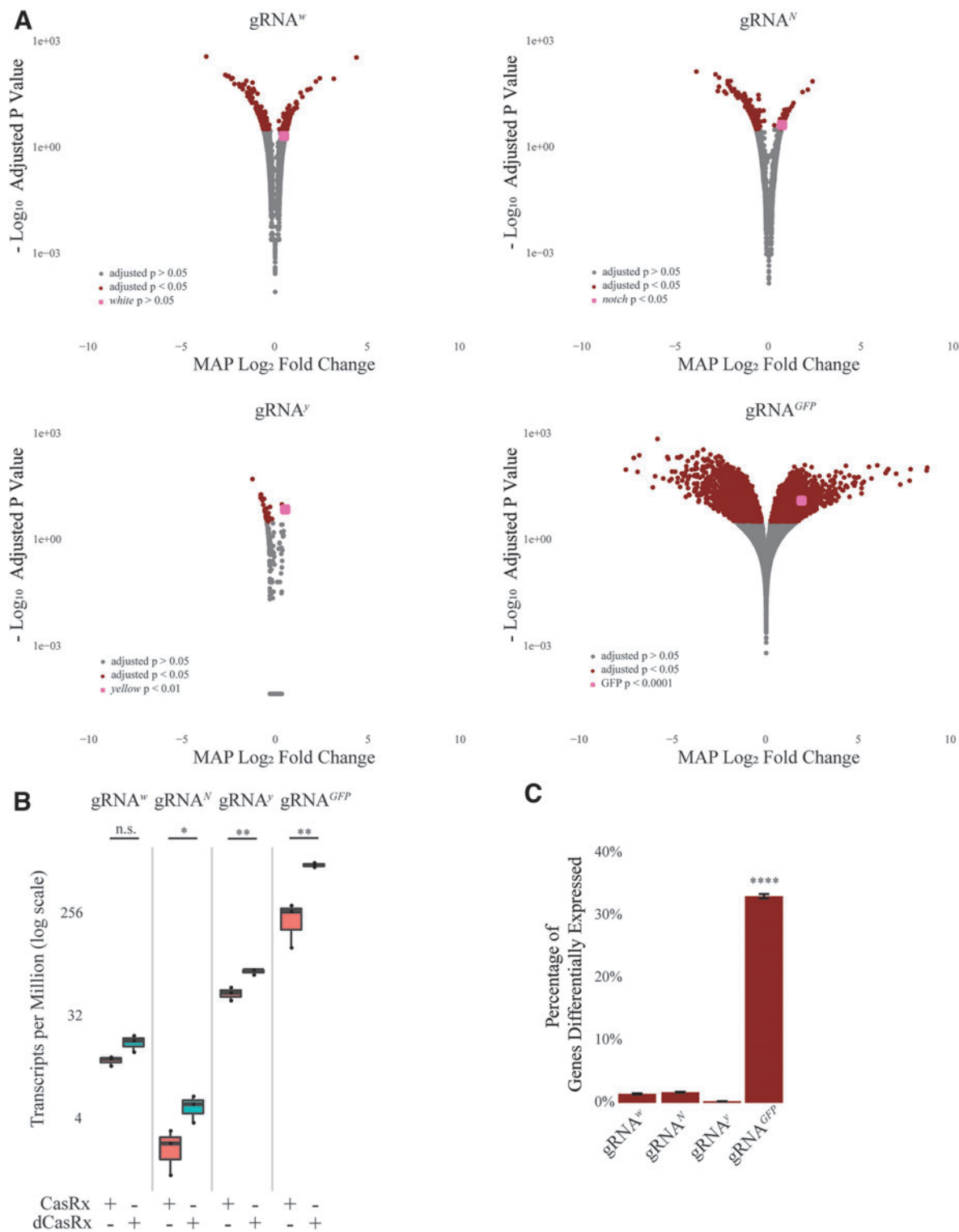


**Fig. 4.** Quantification of potential CasRx-mediated on/off target activity. **(A)** Maximum *a posteriori* estimates for the logarithmic fold change of transcripts. DESeq2 pipeline was used for estimating shrunken Maximum *a posteriori* logarithmic fold changes. Wald test with Benjamini-Hochberg correction was used for statistical inference. Grey dots represent transcripts not significantly differentially expressed between Ubiqu-CasRx and Ubiqu-dCasRx group ( $P > 0.05$ ). Red dots represent transcripts significantly differentially expressed between CasRx and dCasRx group ( $P < 0.05$ ). Pink dot identifies the respective CasRx target gene for each analysis ( $P$ -value indicated in the/by inset). **(B)** Transcript expression levels (TPM) of transcripts targeted with CasRx or dCasRx. Student's *t*-test was used to calculate significance (*w*:  $P = 0.07$ ; *N*:  $P = 0.04$ ; *y*:  $P = 0.006$ ; *GFP*:  $P = 0.008$ ). **(C)** Percentage of transcripts significantly differentially expressed resulting from CasRx cleavage. A pairwise two-sample test for independent proportions with Benjamini-Hochberg correction was used to calculate significance. LFC, logarithmic fold change; MAP, Maximum *a posteriori*.

These results recapitulate previous mechanistic analyses of CasRx and other Cas13 ribonucleases, demonstrating that collateral off-target activity following targeted transcript cleavage is a native feature of Cas13 ribonucleases.<sup>2,4,7–9,51</sup> While this feature may not be desirable for generating tools for targeting specific transcripts of genes, this may be useful for generating sensors that get activated in response to a target transcript (e.g., viral target) such as diagnostic tools that could alert the presence of a nucleic acid target and activate a marker, or even organismal lethality acting as an *in vivo* ribonucleic acid sensor.

Taken together, further optimization will be required to increase the CasRx on-target cleavage rates and decrease cellular toxicity and off-target effects, but this is the first demonstration of a genetically encoded programmable RNA-targeting Cas system in *D. melanogaster*. In the future, optimization of the strength and timing of CasRx expression could mitigate some of the off-target-associated lethality in this system. Stricter and more tunable regulation of CasRx expression may also improve phenotype penetrance as it appears to be dosage dependent in both our system and other CasRx systems.<sup>5</sup> For example, the phenotypes of  $\gamma$  varied by expression, with ubiquitous expression of CasRx resulting in a Ubiqu-CasRx/+; gRNA $\gamma$  /+ lethal phenotype and embryo and wing and body specific expression mitigated lethality phenotype seen in Ubiqu-CasRx expression. Optimization of gRNA design may further improve these systems as CasRx gRNAs have been shown to have variable knockdown efficiency.<sup>5,53</sup> Nevertheless, this is an important first step towards making transcriptome engineering a viable *in vivo* technology and provides a foundation for future experiments to mitigate the off-target and toxic attributes of the enzyme to make a new, viable tool in the expanding gene-editing toolbox.

### Acknowledgments

O.S.A. conceived and designed the experiments. A.B., D.J.B., R.S., and T.Y. performed molecular and genetic experiments. P.H. provided reagents and contributed to the experimental design. All authors contributed to the writing, analyzed the data, and approved the final manuscript.

All constructs generated for this study are available from Addgene (Supplementary Table S2). All fly lines created and/or used in this study are available at the Bloomington Drosophila Stock Center (Supplementary Table S2). Raw sequencing data has been made publicly available at the NCBI SRA submission ID SUB6818910, BioProject PRJNA600654.

### Author Disclosure Statement

O.S.A. and A.B. have a patent pending on this technology. All other authors declare that no competing financial interests exist.

### Funding Information

This work was supported in part by funding from the Defense Advanced Research Project Agency Safe Genes Program Grant (HR0011-17-2- 0047) and a National Institutes of Health New Innovator Award (1DP2AI152071-01) awarded to O.S.A.

### Supplementary Material

Supplementary Figure S1  
 Supplementary Figure S2  
 Supplementary Figure S3  
 Supplementary Figure S4  
 Supplementary Figure S5  
 Supplementary Figure S6  
 Supplementary Table S1  
 Supplementary Table S2  
 Supplementary Table S3  
 Supplementary Table S4  
 Supplementary Table S5  
 Supplementary Table S6  
 Supplementary Table S7  
 Supplementary Table S8  
 Supplementary Table S9  
 Supplementary Table S10  
 Supplementary Table S11  
 Supplementary Table S12  
 Supplementary Table S13  
 Supplementary File S1  
 Supplementary File S2

### References

- Adli M. The CRISPR tool kit for genome editing and beyond. *Nat Commun.* 2018;9:1911. DOI:10.1038/s41467-018-04252-2.
- Abudayyeh OO, Gootenberg JS, Konermann S, et al. C2c2 is a single-component programmable RNA-guided RNA-targeting CRISPR effector. *Science.* 2016;353:aaf5573. DOI:10.1126/science.aaf5573.
- East-Seletsky A, O'Connell MR, Burstein D, Knott GJ, Doudna JA. RNA Targeting by functionally orthogonal type VI-A CRISPR-Cas enzymes. *Mol Cell.* 2017;66:373–383.e3. DOI:10.1016/j.molcel.2017.04.008.
- Konermann S, Lotfy P, Brideau NJ, Oki J, Shokhirev MN, Hsu PD. Transcriptome engineering with RNA-targeting type VI-D CRISPR effectors. *Cell.* 2018;173:665–676.e14. DOI:10.1016/j.cell.2018.02.033.
- Kushawah G, del Prado JA-N, Martinez-Morales JR, et al. CRISPR-Cas13d induces efficient mRNA knock-down in animal embryos. *bioRxiv* 2020 Jan 14 [Epub ahead of print]; DOI:10.1101/2020.01.13.904763.
- Abudayyeh OO, Gootenberg JS, Essletzbichler P, et al. RNA targeting with CRISPR-Cas13. *Nature.* 2017;550:280–284. DOI:10.1038/nature24049.
- Smargon AA, Cox DBT, Pyzocha NK, et al. Cas13b Is a Type VI-B CRISPR-Associated RNA-guided RNase differentially regulated by accessory proteins Csx27 and Csx28. *Mol Cell.* 2017;65:618–630.e7. DOI:10.1016/j.molcel.2016.12.023.
- East-Seletsky A, O'Connell MR, Knight SC, et al. Two distinct RNase activities of CRISPR-C2c2 enable guide-RNA processing and RNA detection. *Nature.* 2016;538:270–273. DOI:10.1038/nature19802.
- Yan WX, Chong S, Zhang H, et al. Cas13d is a compact RNA-targeting type VI CRISPR effector positively modulated by a WYL-domain-containing accessory protein. *Mol Cell.* 2018;70:327–339.e5. DOI:10.1016/j.molcel.2018.02.028.
- Perrimon N, Ni J-Q, Perkins L. In vivo RNAi: today and tomorrow. *Cold Spring Harb Perspect Biol.* 2010;2:a003640. DOI:10.1101/cshperspect.a003640.
- Champer J, Buchman A, Akbari OS. Cheating evolution: engineering gene drives to manipulate the fate of wild populations. *Nat Rev Genet.* 2016;17:146–159. DOI:10.1038/nrg.2015.34.

12. Buchman A, Gamez S, Li M, et al. Broad dengue neutralization in mosquitoes expressing an engineered antibody. *PLoS Pathog.* 2020;16:e1008103. DOI:10.1371/journal.ppat.1008103.
13. Mathur G, Sanchez-Vargas I, Alvarez D, Olson KE, Marinotti O, James AA. Transgene-mediated suppression of dengue viruses in the salivary glands of the yellow fever mosquito, *Aedes aegypti*. *Insect Mol Biol.* 2010;19:753–763. DOI:10.1111/j.1365-2583.2010.01032.x.
14. Franz AWE, Sanchez-Vargas I, Adelman ZN, et al. Engineering RNA interference-based resistance to dengue virus type 2 in genetically modified *Aedes aegypti*. *Proc Natl Acad Sci U S A.* 2006;103:4198–4203. DOI:10.1073/pnas.0600479103.
15. Yen P-S, James A, Li J-C, Chen C-H, Failloux A-B. Synthetic miRNAs induce dual arboviral-resistance phenotypes in the vector mosquito *Aedes aegypti*. *Commun Biol.* 2018;1:11. DOI:10.1038/s42003-017-0011-5.
16. Buchman A, Gamez S, Li M, et al. Engineered resistance to Zika virus in transgenic *Aedes aegypti* expressing a polycistronic cluster of synthetic small RNAs. *Proc Natl Acad Sci U S A.* 2019;116:3656–3661. DOI:10.1073/pnas.1810771116.
17. Dietzl G, Chen D, Schnorrer F, et al. A genome-wide transgenic RNAi library for conditional gene inactivation in *Drosophila*. *Nature.* 2007;448:151–156. DOI:10.1038/nature05954.
18. Ni J-Q, Liu L-P, Binari R, Hardy R, Shim H-S, Cavallaro A, et al. A *Drosophila* resource of transgenic RNAi lines for neurogenetics. *Genetics.* 2009;182:1089–1100. DOI:10.1534/genetics.109.103630.
19. Ni J-Q, Zhou R, Czech B, Liu L-P, Holderbaum L, Yang-Zhou D, et al. A genome-scale shRNA resource for transgenic RNAi in *Drosophila*. *Nat Methods.* 2011;8:405–407. DOI:10.1038/nmeth.1592.
20. Ni J-Q, Markstein M, Binari R, et al. Vector and parameters for targeted transgenic RNA interference in *Drosophila melanogaster*. *Nat Methods.* 2008;5:49–51. DOI:10.1038/nmeth1146.
21. Heigwer F, Port F, Boutros M. RNA interference (RNAi) screening in *Drosophila*. *Genetics.* 2018;208:853–874. DOI:10.1534/genetics.117.300077.
22. Kulkarni MM, Booker M, Silver SJ, et al. Evidence of off-target effects associated with long dsRNAs in *Drosophila melanogaster* cell-based assays. *Nat Methods.* 2006;3:833–838. DOI:10.1038/nmeth935.
23. Ma Y, Creanga A, Lum L, Beachy PA. Prevalence of off-target effects in *Drosophila* RNA interference screens. *Nature.* 2006;443:359–363. DOI:10.1038/nature05179.
24. Perrimon N, Mathey-Prevot B. Matter arising: off-targets and genome-scale RNAi screens in *Drosophila*. *Fly (Austin).* 2007;1:1–5. DOI:10.4161/fly.3601.
25. Markstein M, Pitsouli C, Villalta C, Celniker SE, Perrimon N. Exploiting position effects and the gypsy retrovirus insulator to engineer precisely expressed transgenes. *Nat Genet.* 2008;40:476–483. DOI:10.1038/ng.101.
26. Chakraborty C, Teoh SL, Das S. The smart programmable CRISPR technology: a next generation genome editing tool for investigators. *Curr Drug Targets.* 2017;18:1653–1663. DOI:10.2174/1389450117666160527142321.
27. Jinek M, Chylinski K, Fonfara I, Hauer M, Doudna JA, Charpentier E. A programmable dual-RNA-guided DNA endonuclease in adaptive bacterial immunity. *Science.* 2012;337:816–821. DOI:10.1126/science.1225829.
28. Zuker M. Mfold web server for nucleic acid folding and hybridization prediction. *Nucleic Acids Res.* 2003;31:3406–3415. DOI:10.1093/nar/gkg595.
29. Brand AH, Perrimon N. Targeted gene expression as a means of altering cell fates and generating dominant phenotypes. *Development.* 1993;118:401–415. Available: <https://www.ncbi.nlm.nih.gov/pubmed/8223268> (last accessed June 8, 2020).
30. Gibson DG, Young L, Chuang R-Y, Venter JC, Hutchison CA 3rd, Smith HO. Enzymatic assembly of DNA molecules up to several hundred kilobases. *Nat Methods.* 2009;6:343–345. DOI:10.1038/nmeth.1318.
31. Kandul NP, Liu J, Sanchez C HM, Wu SL, Marshall JM, Akbari OS. Transforming insect population control with precision guided sterile males with demonstration in flies. *Nat Commun.* 2019;10:84. DOI:10.1038/s41467-018-07964-7.
32. Pfeiffer BD, Truman JW, Rubin GM. Using translational enhancers to increase transgene expression in *Drosophila*. *Proc Natl Acad Sci U S A.* 2012;109:6626–6631. DOI:10.1073/pnas.1204520109.
33. Gamez S, Antoshechkin I, Mendez-Sanchez SC, Akbari OS. The developmental transcriptome of *Aedes albopictus*, a major worldwide human disease vector. G3 (Bethesda). 2020;10:1051–1062. DOI: 10.1534/g3.119.401006.
34. Dobin A, Davis CA, Schlesinger F, et al. STAR: ultrafast universal RNA-seq aligner. *Bioinformatics.* 2013;29:15–21. DOI:10.1093/bioinformatics/bts635.
35. Liao Y, Smyth GK, Shi W. featureCounts: an efficient general purpose program for assigning sequence reads to genomic features. *Bioinformatics.* 2014;30:923–930. DOI:10.1093/bioinformatics/btt656.
36. Geyer PK, Green MM, Corces VG. Tissue-specific transcriptional enhancers may act in trans on the gene located in the homologous chromosome: the molecular basis of transvection in *Drosophila*. *EMBO J.* 1990;9:2247–2256. Available at: <https://www.ncbi.nlm.nih.gov/pubmed/2162766> (last accessed June 8, 2020).
37. Akbari OS, Oliver D, Eyer K, Pai C-Y. An Entry/Gateway cloning system for general expression of genes with molecular tags in *Drosophila melanogaster*. *BMC Cell Biol.* 2009;10:8. DOI:10.1186/1471-2121-10-8.
38. Biessmann H. Molecular analysis of the yellow gene (y) region of *Drosophila melanogaster*. *Proc Natl Acad Sci U S A.* 1985;82:7369–7373. DOI:10.1073/pnas.82.21.7369.
39. Sullivan DT, Sullivan MC. Transport defects as the physiological basis for eye color mutants of *Drosophila melanogaster*. *Biochem Genet.* 1975;13:603–613. DOI:10.1007/bf00484918.
40. Kidd S, Kelley MR, Young MW. Sequence of the notch locus of *Drosophila melanogaster*: relationship of the encoded protein to mammalian clotting and growth factors. *Mol Cell Biol.* 1986;6:3094–3108. DOI:10.1128/mcb.6.9.3094.
41. Lindsley DL. Genetic variations of *Drosophila melanogaster* [by] Dan L. Lindsley and E.H. Grell. Washington, DC: Carnegie Institution of Washington, 1968.
42. Port F, Chen H-M, Lee T, Bullock SL. Optimized CRISPR/Cas tools for efficient germline and somatic genome engineering in *Drosophila*. *Proc Natl Acad Sci U S A.* 2014;111:E2967–2976. DOI:10.1073/pnas.1405500111.
43. Michelli CA, Perrimon N. Evidence that stem cells reside in the adult *Drosophila* midgut epithelium. *Nature.* 2006;439:475–479. DOI:10.1038/nature04371.
44. Leonardi J, Fernandez-Valdivia R, Li Y-D, Simcox AA, Jafar-Nejad H. Multiple O-glucosylation sites on Notch function as a buffer against temperature-dependent loss of signaling. *Development.* 2011;138:3569–3578. DOI:10.1242/dev.068361.
45. Simón R, Aparicio R, Housden BE, Bray S, Busturia A. *Drosophila* p53 controls Notch expression and balances apoptosis and proliferation. *Apoptosis.* 2014;19:1430–1443. DOI:10.1007/s10495-014-1000-5.
46. Saj A, Arziman Z, Stempfle D, van Belle W, Sauder U, Horn T, et al. A combined ex vivo and in vivo RNAi screen for notch regulators in *Drosophila* reveals an extensive notch interaction network. *Dev Cell.* 2010;18:862–876. DOI:10.1016/j.devcel.2010.03.013.
47. Massey JH, Chung D, Siwanowicz I, Stern DL, Wittkopp PJ. The yellow gene influences *Drosophila* male mating success through sex comb melanization. *Elife.* 2019;8:e49388. DOI: 10.7554/eLife.49388.
48. Pfeifer TA, Hegedus DD, Griglatti TA, Theilmann DA. Baculovirus immediate-early promoter-mediated expression of the Zeocin™ resistance gene for use as a dominant selectable marker in Dipteran and Lepidopteran insect cell lines. *Gene.* 1997;188:183–190. DOI:10.1016/S0378-1119(96)00756-1.
49. Graveley BR, Brooks AN, Carlson JW, et al. The developmental transcriptome of *Drosophila melanogaster*. *Nature.* 2011;471:473–479. DOI:10.1038/nature09715.
50. Love MI, Huber W, Anders S. Moderated estimation of fold change and dispersion for RNA-seq data with DESeq2. *Genome Biol.* 2014;15:550. DOI:10.1186/s13059-014-0550-8.
51. Meeske AJ, Nakandakari-Higa S, Marraffini LA. Cas13-induced cellular dormancy prevents the rise of CRISPR-resistant bacteriophage. *Nature.* 2019;570:241–245. DOI:10.1038/s41586-019-1257-5.
52. Peretz G, Bakhrat A, Abdu U. Expression of the *Drosophila melanogaster* GADD45 homolog (CG11086) affects egg asymmetric development that is mediated by the c-Jun N-terminal kinase pathway. *Genetics.* 2007;177:1691–1702. DOI:10.1534/genetics.107.079517.
53. Wessels H-H, Méndez-Mancilla A, Guo X, Legut M, Daniloski Z, Sanjana NE. Principles for rational Cas13d guide design. *bioRxiv.* 2019 Dec 28 [Epub ahead of print]. DOI:10.1101/2019.12.27.889089.